COMPUTER SIMULATION OF EFFECT OF CURVED ON DOWNLEAD SURGE ARRESTER IN SUBSTATION ENVIRONMENTS

[1]Salah Mousa [2]Misbah Alhawwari [3]Nafaa Shebani [4]Asheraf Eldieb

[1]Department of Electrical and Electronic Engineering, Sabratha University, Sabratha, Libya
[2]Department of Electrical and Electronic Engineering, Sabratha University, Sabratha, Libya
[3]Department of Electrical and Electronic Engineering, Sabratha University, Sabratha, Libya
[4]Department of Electrical and Electronic Engineering, Sabratha University, Sabratha, Libya

Corresponding Author Email:
Salah.Mousa@Sabu.edu.ly

Abstract:

The performance of surge arresters in high-voltage substations is strongly influenced by the configuration of their downlead conductors, particularly under lightning impulse conditions. International standards recommend that downleads should be as short and straight as possible; however, practical installation constraints often require bends and deviations. This paper investigates the effect of downlead curvature and bending angles on the transient voltage distribution of surge arresters using the Current Distribution, Electromagnetic Interference, Grounding and Soil Structure Analysis (CDEGS) software. A 1.2/50 µs, 10 kA lightning current impulse was injected at the top of a 2.4 m copper downlead connected to a realistic grounding grid embedded in a two-layer soil model. Four configurations were analysed: a straight downlead, a single elbow bend, two elbow bends, and a combined elbow–saddle bend, with bending angles of 10°, 45°, and 90°. The computed results demonstrate that increasing the number and severity of bends leads to significant voltage rises along the downlead, with peak voltage differences exceeding 30 kV for 90° configurations. Additional analytical and numerical evaluations of resistance and inductance confirm that increased curvature introduces higher inductive effects, contributing to the observed voltage amplification. The findings highlight the critical impact of downlead geometry on surge arrester performance and provide quantitative guidance for substation design practices to minimise transient overvoltages and enhance insulation coordination.

Keywords: Surge arrester; Downlead configuration; Lightning impulse; CDEGS simulation; Grounding system; Inductance effect; Substation earthing; Transient overvoltages

1. Introduction:

Earthing systems are designed to disperse into ground high magnitude currents caused by abnormal and system fault conditions and provide protection to people working in or living close to power system installations. It is essential that earthing systems are designed with low-magnitude earth impedance so that the high value and fast transient surges are conducted to ground effectively. High voltage distribution and transmission systems are protected from lightning by surge arresters requiring low impedance connection to earth at high frequencies. In power substations, buried earth grid, vertical rods and horizontal electrodes are used in combination to obtain a low impedance connection to earth.

The characteristics of an earthing systems under lightning conditions differ from those at power frequency, and the earthing system must be designed to operate satisfactorily under all conditions. At high frequencies, the performance of the earthing system will be influenced by inductive and capacitive effects. For example, the inductance of a small earthing system such a rod dominates the high frequency impedance characteristic, thereby lowering its effective length.

A recommendation common to all the standards is that the earth connection between substation equipment involved in the dissipation of surges and the buried earth electrode system should be of low resistance and reactance, and to achieve this it should be as short and as straight as possible [2-8]. For surge arresters, it is also recommended that the live connection to the protected primary plant should also be as short and straight as possible and, therefore, surge arresters should be situated as close as possible to the equipment being protected. In addition, the connection lead from the surge arrester to the busbars conductors should have a small angle towards the equipment between (-20^0 to -30^0) [3-5]. A careful selection of material being used in downlead conductor must been made based on the environmental circumstances. It implies that, for the sulphates-concentrated environment, either copper or aluminium is recommended due to their great conductivity [8]. However, aluminium is inappropriate when used in earthing or implanted in concrete as a copper material. [8]. As such, copper-type was chosen in this investigation.

Hence, this study is to investigate the bending degree effect on downleads studies for surge arrester were carried out by constructing simulation models Simulation of surge arresters in substation environments using CDEGS.

2. Computer Simulation

The Current Distribution, Electromagnetic Interference, Grounding and Soil Structure Analysis (CDEGS) 'Hifreq' and 'FFTSES' computer program was used for these studies. As shown in figure1, a 1.2/50 current surge is assumed, with a 10kA lightning current is injected at the top of the downlead of the surge arrester.

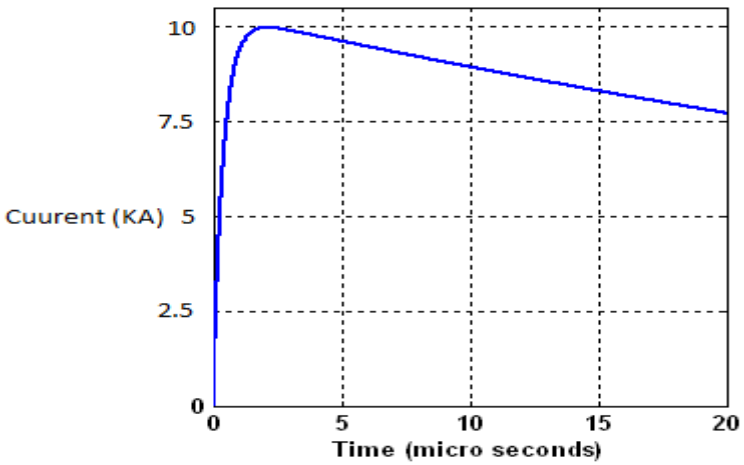

Fig.1: Impulse lightning current 10kA with rise time of 1.2/50μs

The total height of a 2.4m in all cases with cross-sectional area of $50mm^2$ was used for these studies. A two-layer soil model was adopted for the simulations with a top layer having a depth of 8.6m and resistivity 143Ω.m and bottom layer with a resistivity of 62Ω.m. Also, an 100m×100m grid, buried at a depth of 50 cm was used as grounding system. The computations

of the voltages in all cases using CDEGS were carried out between six to eight important points (V_0 to V_6) for the downlead of surge arresters using different scenarios for the downlead bending, as shown in Figure 2. These are:

- Scenario 1: Straight downlead (0^0 angle)
- Scenario 2: The downlead has a single elbow bend ($10^0/45^0/90^0$) at approximately 1.1m from the ground surface.
- Scenario 3: Two elbow bends ($10^0/45^0/90^0$) at both the top of the downlead and at approximately of 1.1m from the ground surface.
- Scenario 4: An elbow bend ($10/45/90^0$) at the top of the download, and saddle bend ($10^0/45^0/90^0$) at roughly 1.1m from the ground surface.

Figure 3 shows examples of computed waveshapes at nodes V_0 (ground surface) to V_5 (at injection point) when a 1.2/50, 10kA surge was injected at the top for scenario I. It can be seen from the figure that the distribution of voltage along the downlead is uniform, and the voltage difference between two points V_1 and V_2 is 8kV. However, from Figure 4, the difference voltages between V_1 and V_3 for scenario II are 16kV, 21kV and 23kV for angles 10^0, 45^0 and 90^0, respectively. Figure 5 presents the results for the scenario III. For Scenario III where the bending is increased, and the voltage differences for angles 10^0, 45^0 and 90^0, computed between points V_2 and V_4 (before and after the bending) for are 15kV, 22kV and 23kV. In this scenario IV, as shown in Figure 6, these voltage differences between V_2 and V_5 for the same angles reach 19kV, 28kV and 31kV, respectively. All results are tabulated in Table 1.

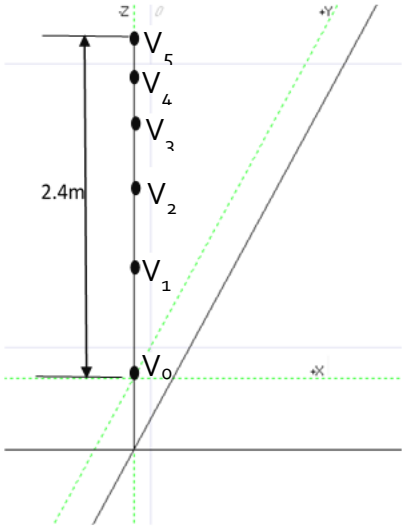

a) Scenario I: Straight downlead

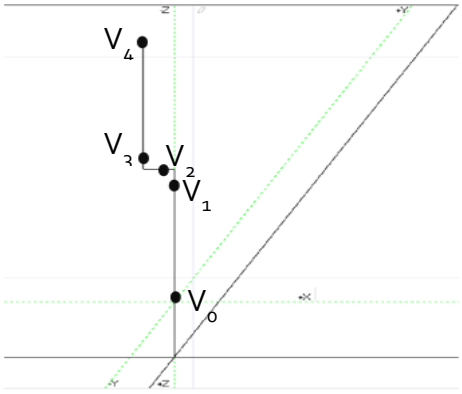

90°

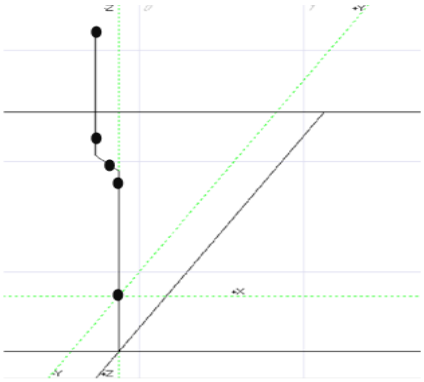

45°

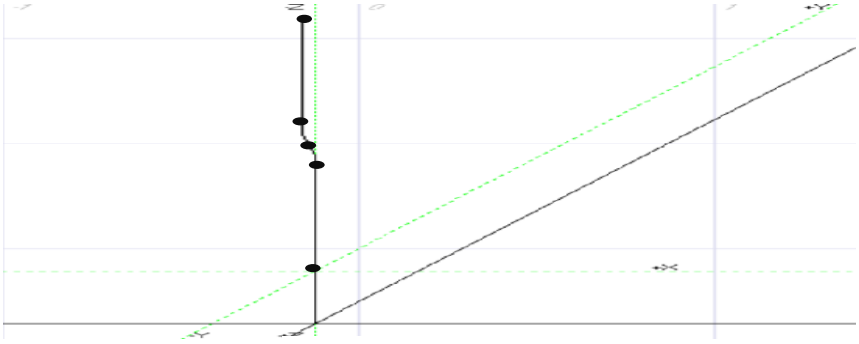

10°

b) Scenario II: Single elbow bend

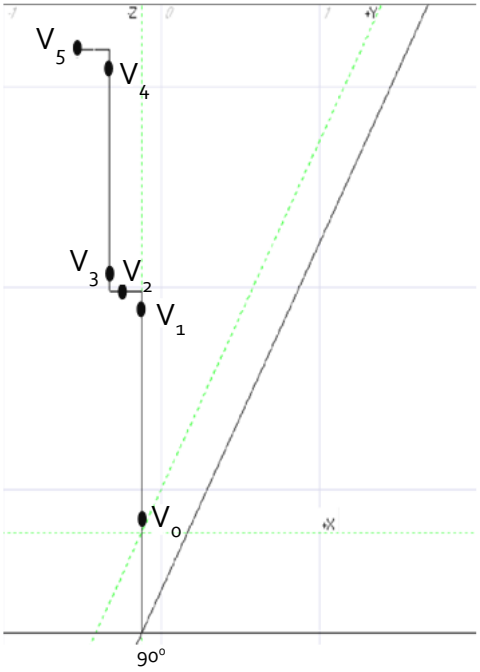

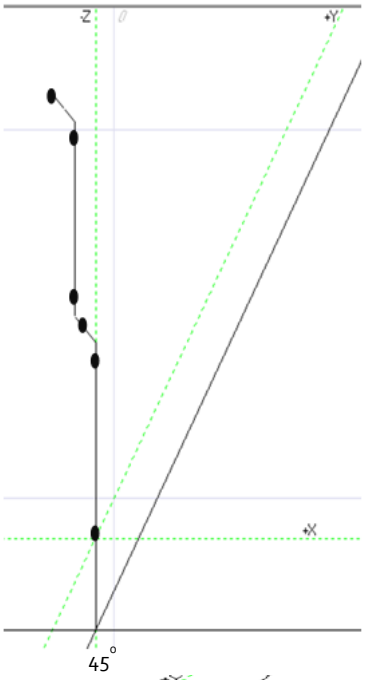

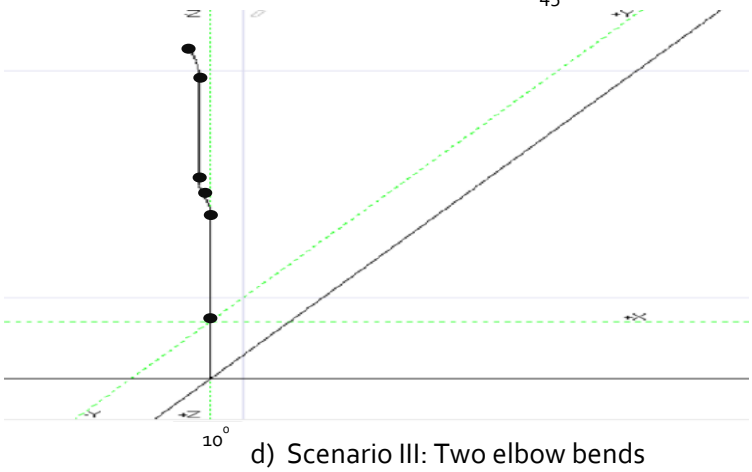

d) Scenario III: Two elbow bends

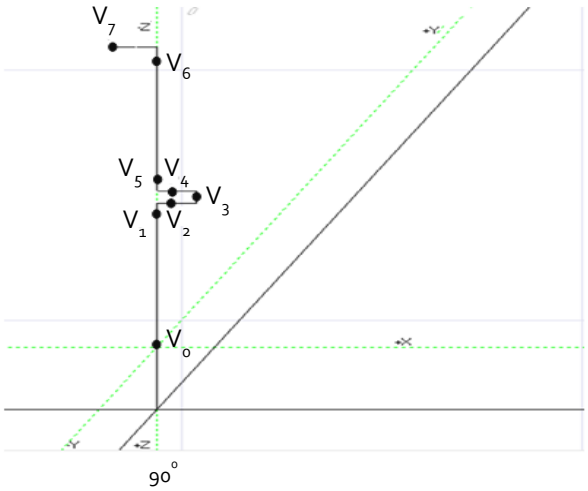

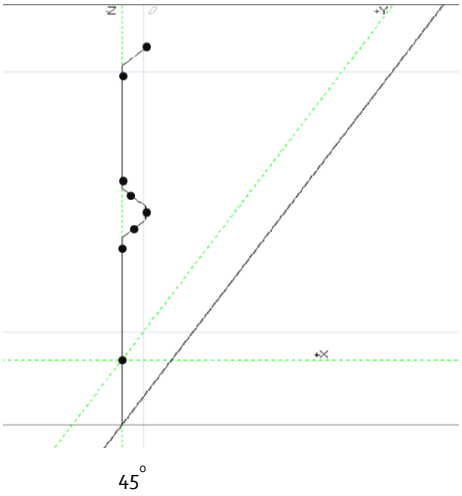

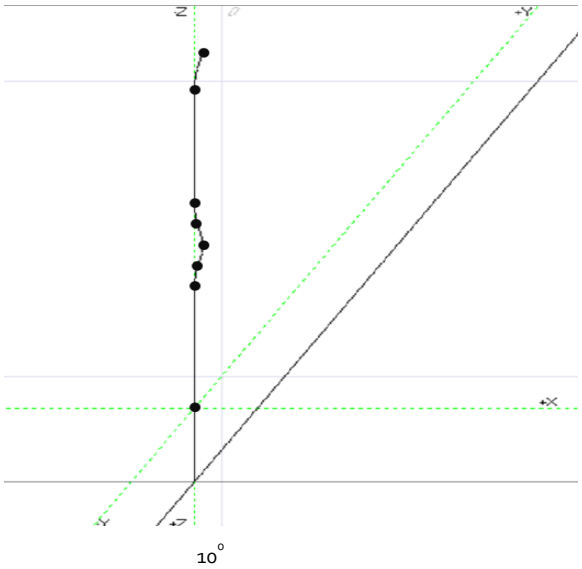

e) Scenario IV: Elbow and saddle bends

Fig.2: Four scenarios I, II, III, and IV used for CDEGS modelling.

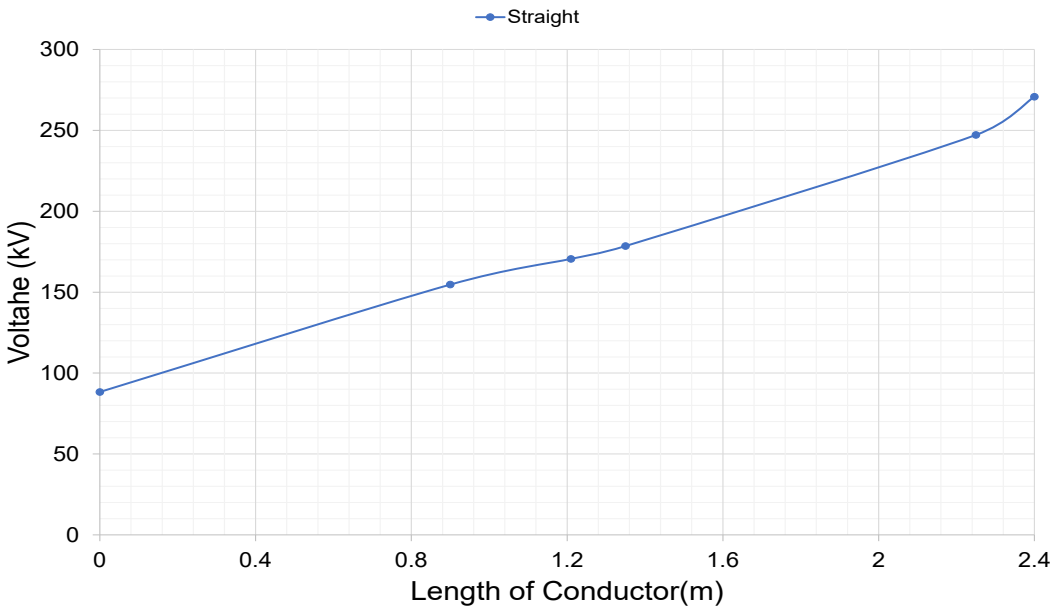

Fig3: Voltage magnitudes for scenario I

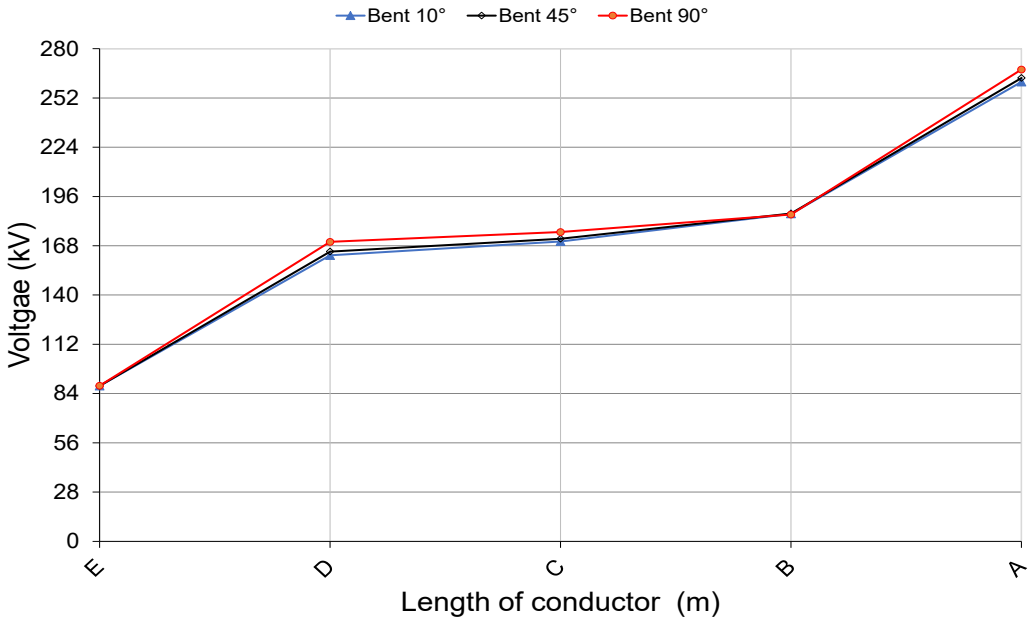

Fig.4: Voltage magnitudes for scenario II

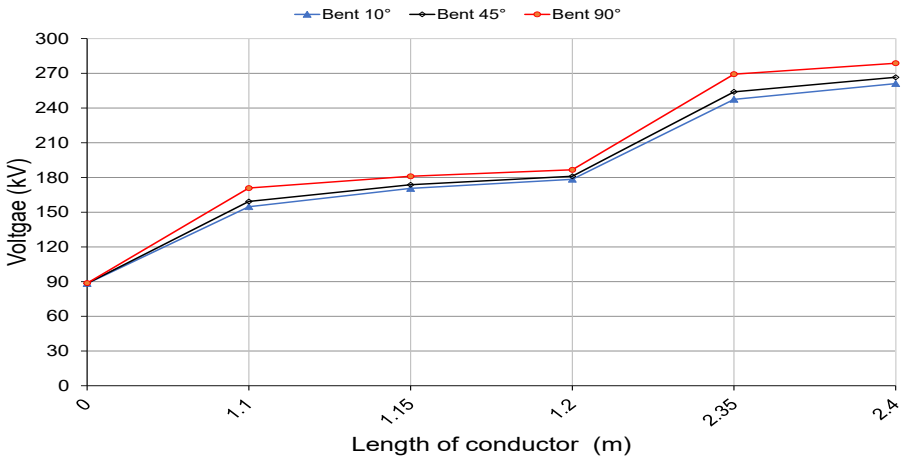

Fig.5: Voltage magnitudes for scenario III

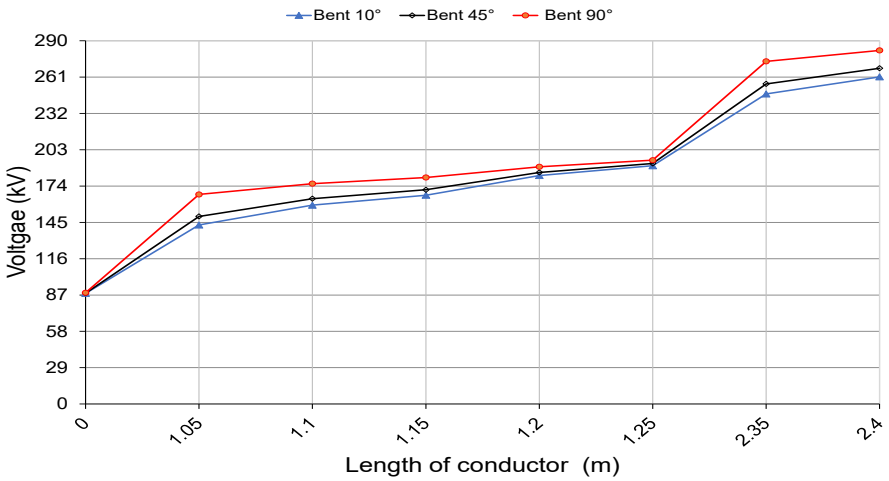

Fig.6:Voltage magnitudes for scenario IV

Table 1: voltages computed by CDEGS for scenario I

Position (m)	Voltage point	Voltage(kV)
0	V_0	88
0.90	V_1	155
1.21	V_2	171
1.35	V_3	179
2.25	V_4	247
2.40	V_5	271

Table 2 presents the voltages calculated using CDEGS software for Scenario II at different distances and angular conditions. The results indicate an overall increase in voltage with increasing distance, from 88 kV at the reference point (V_0) to a maximum of 268 kV at (V_4) under the (90^0) condition. The influence of the angular condition is relatively limited, with a maximum difference of 7 kV between the (10^0) and (90^0) cases. Identical voltage values are obtained at (V_0) and (V_3) for all three angles, whereas small variations are observed at the other points. These findings demonstrate that the calculated voltage varies with both distance and angular condition under Scenario II.

Table 2: voltages computed by CDEGS for scenario II

Distance	Voltage point	Voltage (kV)		
		10^0	45^0	90^0
0	V_0	88	88	88
1.1	V_1	163	165	170
1.52	V_2	170	172	176
1.55	V_3	186	186	186
2.4	V_4	261	263	268

Table 3 presents the voltages computed using CDEGS (Current Distribution, Electromagnetic Fields, Grounding and Soil Structure Analysis software) for a specific operating condition designated as Scenario III. It details how voltage magnitudes change across various distances (V_0 to V_5) at three distinct angular orientations (0^0, 10^0, 45^0, and 90^0).

The results for Scenario III demonstrate that computed voltages increase steadily as distance from the reference point increases, reaching a maximum of 279 kV at distance 1.25 (90^0). Furthermore, the data shows a clear directional dependency, where higher angles consistently yield higher voltage magnitudes at equivalent distances.

Table 3: voltages computed by CDEGS for scenario III

Distance	Voltage point	Voltage (kV)		
		10^0	45^0	90^0
0	V_0	88	88	89
1.05	V_1	155	159	171
1.1	V_2	171	174	181
1.15	V_3	178	181	187
1.2	V_4	248	254	269
1.25	V_5	261	267	279

3. Calculation of Resistance and Inductance of the Downlead conductor

I. Linear resistance

Figure 8 shows the geometry views in COMSOL for different configurations. Assuming a cross section of 5x50mm and a volume resistivity of copper of $1.68 \times 10^{-8} \Omega m$, we get a DC resistance of:

$$R'_{dc} = \frac{\rho}{wt} = 67.2 \mu\Omega m^{-1} \qquad (1)$$

A 2.4m straight downlead will have a dc resistance not less than $161\mu\Omega$, the ac resistance of the bar will be:

$$R'_{ac} = \frac{\rho}{\delta(2t - 4\delta + 2w)} \qquad (2)$$

Where:

$$\delta = \sqrt{\frac{\rho}{\pi f \mu_0}} \qquad (3)$$

At 10kHz: $R'_{ac} \approx 239 \mu\Omega m^{-1} \rightarrow \ R = 573 \mu\Omega$
At 100kHz: $R'_{ac} \approx 744 \mu\Omega m^{-1} \ \rightarrow \ R = 1.97 m\Omega$
At 1MHz: $R'_{ac} \approx 2.34 m\Omega m^{-1} \ \rightarrow \ R = 5.62 m\Omega$

II. Calculation of Inductance

Equations reproduced from inductance calculations by Grover []

a. Inductance of a Straight Rectangular Bar

$$L = 2l\left[\ln\frac{2l}{\alpha+\beta} + \frac{1}{2} + \frac{0.2235(\alpha+\beta)}{l}\right] \times 10^{-7}\ H \qquad (4)$$

Where l is the length of the straight section, α is the thickness, and β the width. For a 2.4m straight bar, with width 50mm and thickness 5mm, we have 2.39uH. At high frequencies this drops to no less than 2.2uH, so a good approximation is found by assuming $1 \mu H m^{-1}$ for straight downleads.

b. Inductance of Straight bar with 90° deviations

For the 90-degree deviations, we can add to our straight bar calculation an antiparallel pair of bars of length l =20cm, with a geometric mean distance d = 10cm, L is calculated using (1), and the mutual inductance is:

$$M = 2\left[l \ln\frac{l + \sqrt{l^2 + d^2}}{d} - \sqrt{l^2 + d^2} + d\right] \times 10^{-7} H \qquad (5)$$

Therefore L_1 is 102nH and M is 33nH. The resulting additional inductance is:

$$L = 2(L_1 - M) \qquad (6)$$

Giving an additional inductance of $138nH$, for a total of 2.53uH. Not that the inductance is lower than would be expected by linear approximation.

For angles in between, the calculation is not simple, and an intermediate value is assumed as a first approximation ($L = 2.39 + 0.138\sin(\theta)$). Evaluation of L for an open-ended conductor in COMSOL is impossible due to the constraint of the maxwell formulation. As the simulation domain is expanded, the effective current loop increases, increasing L. A domain was chosen to replicate the inductance of the straight conductor and kept constant for all other configurations. Table 4 includes the calculation of the inductance. The inductance is then approximated from the magnetic energy density:

$$L \approx \frac{2}{I^2}\int_V W_m \qquad (7)$$

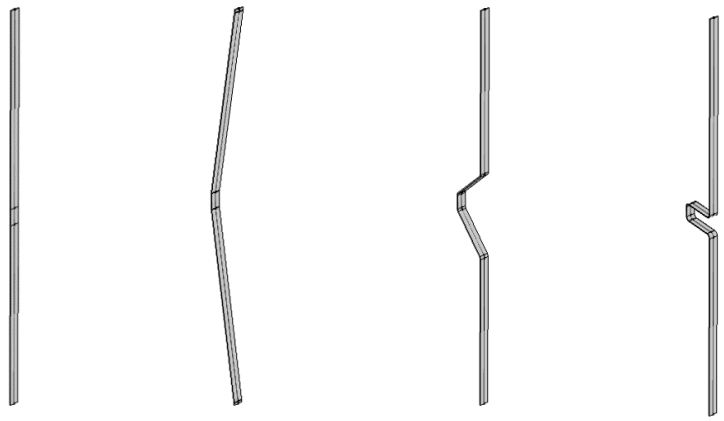

Figure 7: Geometry views in COMSOL for configurations 0°/10°/45°/90° - total height =2.4m in all cases

The table 4 demonstrates a strong correlation between analytical and numerical results, confirming the validity of the hand calculation approach. The gradual increase in inductance with angle and the small differences between the two methods highlight the reliability of the simulation while also revealing the limitations of analytical approximations at higher angles.

Table 4: Inductance calculations by hand and numerical simulation

Angle	Hand Calculation (uH)	COMSOL Calculation (uH)
0	2.39	2.39
10	2.41	2.40
45	2.48	2.47
90	2.53	2.48

4. Conclusion:

This paper has presented a comprehensive numerical investigation into the influence of downlead geometry on the transient performance of surge arresters under lightning impulse conditions. Using the CDEGS simulation platform, various practical downlead configurations were analysed, including straight conductors, single and multiple elbow bends, and combined elbow–saddle arrangements with bending angles ranging from 10° to 90°. A realistic substation grounding system and two-layer soil model were adopted to ensure that the results reflect practical installation conditions.

The simulation results clearly demonstrate that deviations from a straight downlead significantly affect the voltage distribution along the surge arrester connection. As the number of bends and the bending angle increase, substantial voltage rises occur at locations immediately before and after the bends. For severe configurations involving 90° bends, peak voltage differences exceeding 30 kV were observed when compared to the straight downlead case. These elevated voltages are primarily attributed to the increased inductive effects introduced by curvature, which become dominant under fast-front lightning impulses.

Analytical and numerical evaluations of resistance and inductance further support the simulation findings. While changes in resistance were shown to be relatively small, even modest increases in inductance due to downlead bending were sufficient to produce pronounced voltage amplification at high frequencies. The combined use of hand calculations and COMSOL-based numerical estimations confirmed a consistent rise in inductance with increasing bending severity, validating the physical interpretation of the CDEGS results.

Overall, the study confirms that downlead geometry is a critical factor in surge arrester performance and insulation coordination in high-voltage substations. The findings strongly reinforce existing international standards recommending that downleads should be as short and as straight as possible, while also providing quantitative evidence of the risks associated with unavoidable bends. The results offer practical guidance for substation designers and engineers, highlighting the importance of minimising downlead curvature to reduce transient overvoltage, improve lightning protection effectiveness, and enhance the overall reliability and safety of power system installations.

5. References

[1] EA 41-24 (1992) Guidelines for the design, installation, testing and maintenance of main earthing systems in substations, Electricity Association, London.
[2] IEEE 80 (2000) Guide for safety in ac substation grounding, IEEE Standards Department.
[3] BS 7354 (1990) Code of Practice for Design of high-voltage open-terminal stations, British Standards Institution, London.
[4]IEEE 142 (1991) IEEE Recommended Practice for Grounding of Industrial and Commercial Power Systems, IEEE Standards Department, New York.
[5] EA 41-24, (1992), "Guidelines for the design, installation, testing and maintenance of main earthing systems in substations", Electricity Association, London, 1992
[6] BS 7430 (1998) Code of Practice for Earthing, British Standards Institution, London.
[7]CENELEC HD 637 S1 (1999) Power installations exceeding 1kV a.c., CENELEC Harmonization Document.
[8]MS IEC 62305-3 (2007) Protection Against Lightning Part 3: Physical Damage To Structures and Life Hazard.